

Elastic and Shear Moduli of Single-Walled Carbon Nanotube Ropes

Jean-Paul Salvetat,^{1,*} G. Andrew D. Briggs,² Jean-Marc Bonard,¹ Revathi R. Bacsa,¹ Andrzej J. Kulik,¹

Thomas Stöckli,¹ Nancy A. Burnham,¹ and László Forró¹

¹*Département de Physique, Ecole Polytechnique Fédérale de Lausanne, CH-1015 Lausanne, Switzerland*

²*Department of Materials, Oxford University, Parks Road, Oxford OX1 3PH, Great Britain*

(Received 17 June 1998)

Carbon nanotubes are believed to be the ultimate low-density high-modulus fibers, which makes their characterization at nanometer scale vital for applications. By using an atomic force microscope and a special substrate, the elastic and shear moduli of individual single-walled nanotube (SWNT) ropes were measured to be of the order of 1 TPa and 1 GPa, respectively. In contrast to multiwalled nanotubes, an unexpectedly low intertube shear stiffness dominated the flexural behavior of the SWNT ropes. This suggests that intertube cohesion should be improved for applications of SWNT ropes in high-performance composite materials. [S0031-9007(98)08306-9]

PACS numbers: 61.48.+c, 61.16.Ch, 62.20.-x

It has been known for some time that carbon nanotubes have remarkable electrical properties [1]. It is becoming increasingly apparent that they also have astonishing mechanical properties, and that they provide a way of exploiting the enormous strength associated with sheets of graphite in a fiber geometry.

All of the benefits associated with composite design could thus be implemented on the nanoscale, with what are probably the strongest fibers available to mankind. In order to do this intelligently, it is vital to understand the mechanical behavior of nanotubes. Theoretical [2] and experimental [3] studies have shown that single multiwalled nanotubes (MWNTs) can undergo enormous bending deformation and recover apparently elastically. Several recent papers have shown that MWNTs are extremely rigid rods of very low density with unique mechanical properties [3–6]. These properties depend critically on the arrangement of the graphitic planes [6], which confirms that MWNTs, as long as the graphitic planes are aligned with the tube axis, maximize the effect of the very high in-plane elastic constant of graphite.

In contrast to MWNTs, single-walled nanotubes (SWNTs) are formed of only one rolled-up graphene sheet. They lack the multiple cylindrical nesting of MWNTs and should have even better mechanical properties due to curvature effects. In fact, an additional stiffening of the curved graphene sheets is predicted when the radius is lower than 0.5 nm [7], due to the strain caused by wrapping. Furthermore, SWNTs are mostly arranged in ropes with a close-packed stacking, which thus form self-assembled cables on the nanometer scale and could be the ultimate high-modulus fibers [8]. We report here on the first measurement of the elastic properties of crystalline SWNT ropes.

Crystalline ropes of SWNTs were produced by the arc-discharge method [9] and purified by acid treatment and filtration [10]. Recent high-resolution transmission electron microscopy (HRTEM) and Raman studies [11] show that a narrow diameter distribution is achieved with

a proper choice of catalyst. The mean diameter of our nanotubes is about 1.4 nm, and the diameter of the bundles ranges from 3 to 20 nm with a length of several microns. Figure 1(a) shows a HRTEM image of a typical SWNT rope. The view in the cross section of Fig. 1(b) reveals that the tubes are arranged in a close-packed lattice. Because the ropes are composed of tubes of different diameters and helicities, local distortions of the lattice are to be expected. Furthermore, tubes can also be missing in a rope, resulting in vacancies in the tube lattice [12].

For direct measurements of the elastic properties of SWNT ropes, the purified soot was dispersed in ethanol and a droplet was deposited on a polished alumina ultrafiltration membrane (Whatman Anodisc, with 200 nm pores). Nanotubes occasionally lie over pores with most

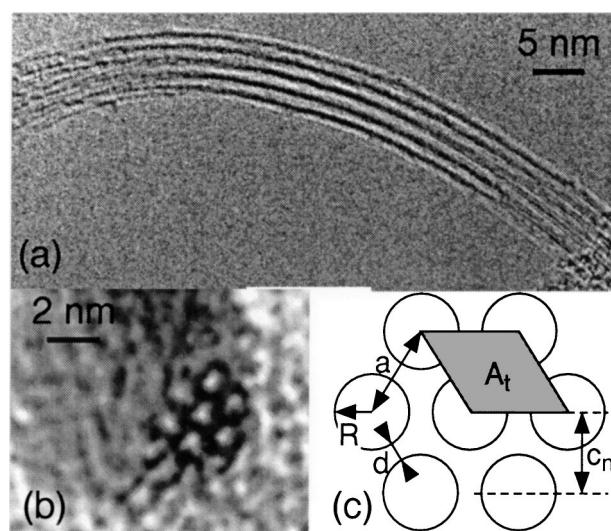


FIG. 1. (a),(b): High-resolution transmission electron microscopy images of SWNT ropes. (a) shows a 6 nm diameter rope. (b) shows a cross section of a rope as it bends in and out of the focal plane of the microscope. (c) is a schematic of the tube lattice with the different parameters used in the first order model.

of the tube in contact with the membrane surface, producing a suspended beam configuration at the nanoscale. Figure 2(a) shows a SWNT rope of 20 nm diameter suspended over a 200 nm pore. An atomic force microscope (AFM) operating in air was used to apply a load to the nanobeams and to determine directly the resulting deflection [as indicated in the schematics of Fig. 2(b)].

The deflection of a beam resulting from a force applied midway along its suspended length depends critically on the boundary conditions, i.e., on the manner in which the extremities of the beam are attached [13]. If the beam is simply supported, the slopes at both extremities of the suspended portion are finite, whereas they are zero if the beam is clamped. In our case, adhesion of the ropes on the substrate and between the tubes in a rope was sufficiently strong to prevent any lift-off, providing a clamped beam configuration [14]. The deflection versus applied force measurements showed that the nanotube response was linear and elastic for the range of applied forces (up to 3 nN). No permanent deformation of the ropes was detected.

In order to determine the elastic properties from deflection versus force measurements, we determined the suspended length and the cross-sectional area of the rope. The former parameter can be determined by comparing deflection profiles acquired on, and just beside, the suspended rope. As for the latter, it is related to the square of the height for cylindrical objects such as MWNTs. For a rope, which can have a rectangular or trapezoidal cross section, the width must be measured in addition to the

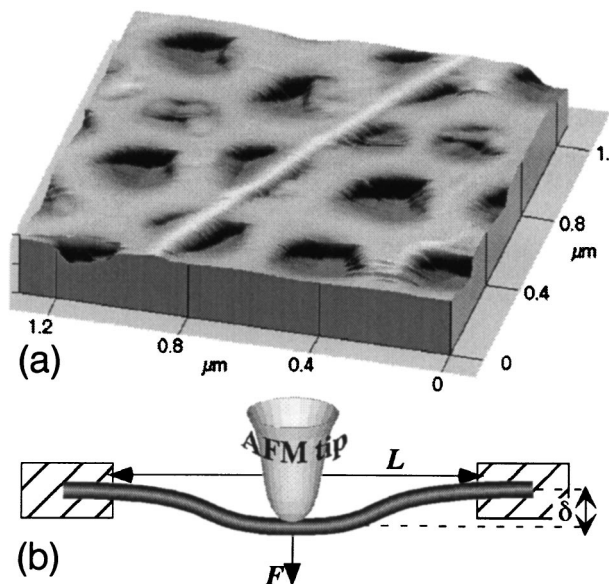


FIG. 2. (a) AFM image of a SWNT rope adhered to the polished alumina ultrafiltration membrane, with a portion bridging a pore of the membrane. (b) Schematic of the measurement: the AFM is used to apply a load to the nanobeam and to determine directly the resulting deflection. A closed loop feedback ensured an accurate scanner positioning. Si_3N_4 cantilevers with force constants of 0.05 and 0.1 N/m were used as tips in the contact mode.

height. In an AFM image, the apparent rope width is a combination of tube diameter and tip radius and hence gives a poor estimate of the actual lateral dimension of the rope. To solve this problem we calibrated the SWNT rope profiles with cylindrical MWNT of equivalent diameters using the same tip, and we selected ropes with nearly symmetrical profiles. The exact cross section is intermediate between a square and a cylinder. In the following, we assume that the ropes are cylindrical, taking the resulting error into account in the overall error. In fact, the height H of a crystalline hexagonal bundle clamped onto the substrate takes discrete values: $H = 2R + a\sqrt{3}/2(N - 1)$, where N is the number of layers, R is the mean radius of the SWNT comprising the rope, and a is the lattice constant of the rope [see Fig. 1(c)]. H increases therefore in steps of ~ 1.5 nm, which is in good agreement with our experimental findings. This fact was used for enhancing the precision of the measured height for small ropes (3 and 4.5 nm) since the precision of the AFM is limited to ± 0.5 nm in our case. The force-deflection results are summarized in Table I.

From simple considerations, one can expect the elastic modulus of SWNTs to be of the order of the in-plane modulus of graphite, i.e., about 1 TPa. The most simple model for a SWNT rope is to consider the tubes to be independent of one another: In this case, the elastic modulus is calculated by applying the usual clamped beam formula for a single tube with the applied force divided by the number of tubes in the rope. However, the modulus deduced in this way would be higher than 10 TPa for our data, far higher than the most optimistic predictions. Thus SWNT ropes cannot be simply taken as an assembly of free tubes; rather, the ensemble of tubes must be considered as one anisotropic beam.

In the general case, deflection of beams involves both bending and shear deformations. The superposition principle implies that the total deflection, δ , is the sum of the deflections due to bending, δ_B , and to shear, δ_S . If we use the unit-load method for a concentrated load F , the deflection at the middle [13] becomes

TABLE I. Diameter D , suspended length L , slope of the force-deflection curve $\Delta\delta/\Delta F$, as well as the calculated reduced modulus E_r and shear modulus G for the SWNT ropes studied in this work.

D (nm)	L (nm)	$\Delta\delta/\Delta F$ (m/N)	E_r (GPa)	G (GPa)
± 0.5 nm	$\pm 10\%$		$\pm 50\%$	$\pm 50\%$
3.0	100	1.0	1310	...
3.0	140	4.0	899	...
4.5	285	9.3	642	...
4.5	180	3.0	503	6.5
6.0	200	1.8	369	2.9
6.0	230	3.0	332	1.7
9.0	180	0.5	189	2.3
13.5	360	0.5	298	2.8
13.5	360	1.0	149	0.9
20.0	370	0.5	67	0.7

$$\delta = \delta_B + \delta_S = FL^3/192EI + f_s FL/4GA, \quad (1)$$

where L is the suspended length, E is the elastic modulus, f_s is the shape factor (equal to $10/9$ for a cylindrical beam), G is the shear modulus, I is the second moment of area of the beam ($I = \pi D^4/64$ for a filled cylinder), and A is the cross-sectional area. The ratio δ_B/δ_S increases with the ratio of beam length to diameter. When G and E are of comparable magnitude, shear effects become important only for relatively short beams. In nanoropes, we expect a non-negligible contribution of shear even for long beams, which will increase the deflection and lower the apparent E value. In fact, shear becomes an important contribution when $L/R \leq 4\sqrt{E/G}$ [13]. The pure bending formula ($\delta = \delta_B$) for determining E will apply only for long ropes of small diameter.

The effect of shearing is emphasized by the variation of $FL^3/192\pi\delta D^4$ as a function of rope diameter D . We call this parameter the “reduced modulus,” E_r . As discussed above, E_r is equal to the elastic modulus when shearing is negligible, which is the case, for example, for MWNT [6]. In Fig. 3 and Table I, we show the measured reduced modulus for ten different SWNT ropes with diameters comprised between 3 and 20 nm. For small long ropes, we deduce an elastic modulus of about 1 TPa, which is in agreement with the measurements by electron microscopy performed by Chopra and Zettl on a single SWNT [15]. However, the reduced modulus depends strongly on the diameter of the ropes, decreasing by more than 1 order of magnitude from 3 to 20 nm.

In the following, we attempt to model the trend observed in Fig. 3 using theoretical considerations. It is to be expected that the tensile stiffness of the nanoropes

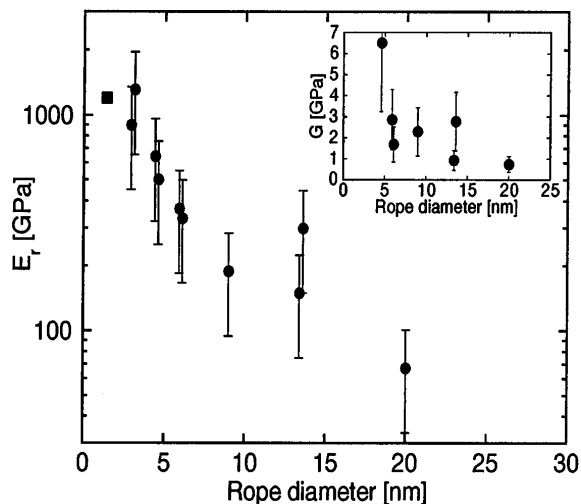


FIG. 3. Measured reduced modulus, E_r , for ten different SWNT ropes with diameters between 3 and 20 nm (circles). The points corresponding to different ropes of equal diameters have been shifted by ± 0.2 nm for better legibility. The value obtained by Chopra *et al.* [15] for a single nanotube is plotted for comparison (square). Inset: Shear modulus for large ropes ($D > 4$ nm) extracted for the experimental data by assuming $E = 600$ GPa.

will be similar to that of individual nanotubes. With this assumption, the elastic modulus normalized by the cross-sectional area should be the same for all ropes. However, the shear modulus in ropes may be quite different from that of single nanotubes, because in the latter the shear modulus of the tube wall is equal to the graphitic elastic constant $c_{66} = 1/2(c_{11} - c_{12}) = 330$ GPa, whereas in the former it will be dominated by shear between individual nanotubes. As a rough model, we suppose that individual tubes are arranged in a 2D close-packed regular array of lattice constant $a = 2R + d$ [Fig. 1(c)], where d is the intertube distance, which amounts to ~ 3.4 Å [16]. The cross-sectional area occupied by each tube is $A_t = a^2 \cos \pi/6$, with a circumference $C_t = 2\pi R$.

To first approximation, the strength of the in-plane chemical bond is similar for a graphitic plane and for a SWNT, which has been confirmed by simulations [8,17]. Hence, the in-plane sheet stiffness should be the same for bulk graphite and for a SWNT. A SWNT that occupies a cross-sectional area A_t in a rope is equivalent to a plane of sp^2 -bonded carbon atoms of width C_t and “thickness” c , where c is the interplanar spacing of graphite ($c = 3.354$ Å). We can thus estimate the elastic modulus of the rope, E_{rope} , by taking $E_{\text{rope}}A_t = cCE_{\text{graphite}}$, i.e., $E_{\text{rope}} = c(C/A_t)E_{\text{graphite}}$, which yields a value of $E_{\text{rope}} \approx 600$ GPa.

For the shear modulus, if we neglect the shearing of individual tubes, $G_{\text{rope}} = (c_n/c)G_{\text{graphite}}$, where c_n is the distance between two tube layers ($c_n = a \cos \pi/6$) [Fig. 1(d)]. If we take $G_{\text{graphite}} = 4.5$ GPa (c_{44} of single crystal graphite), we obtain $G_{\text{rope}} \approx 19.5$ GPa. Note that, owing to the high nanotube shear modulus, the global shear modulus of a rope increases compared to planar graphite.

From small diameter long ropes, in which shearing is negligible, the elastic modulus we measured is in close agreement with the above model and also with the more elaborate calculation of Lu [8]. The high value of E for the 3 nm ropes is probably due to an underestimation of the rope area, arising from the uncertainty in the lateral dimension. We can expect E to be nearly constant for all ropes, i.e., independent of the diameter, since E depends on the stiffness of the single-walled tubes which compose the rope. However, we cannot rule out the possibility that some tubes are interrupted in the middle of the ropes. High-resolution transmission electron microscopy images also show that some tubes can be missing in a rope, producing vacancies in the tube lattice. For this effect to be significant on E , a large proportion of tubes should be missing or interrupted. In that case, the rope would be easily distorted by the AFM tip on the portion lying on the membrane. The profile and diameter of SWNT ropes remained unchanged when imaged with different forces, suggesting that the effect of vacancies on E , if present in the measured portion of a rope, is rather small.

By taking $E = 600$ GPa, we can extract the shear modulus for large ropes ($D > 4.5$ nm) with Eq. (1) as

shown in the inset of Fig. 3 and in Table I. The shear modulus G determined in this way is lower than predicted by the first order model; G shows a fairly large dispersion, and decreases for large diameter ropes. By analogy with graphite, intertube shear effects are expected to be sensitive to the various imperfections that may be present in the ropes. In pyrographites or highly oriented pyrolytic graphite, the apparent c_{44} value can be as low as 0.2 GPa [18] due to the presence of gliding basal plane dislocations and stacking faults. Such an effect of dislocations is typical of graphite because of its large anisotropy. In isotropic metals, anelastic effects are far less pronounced. In SWNTs, pentagon-heptagon pairs are equivalent to dislocations but they do not glide easily and should have only a small influence on G in a rope. In fact, it is probable that this lowering of G is due mostly to structural imperfections, e.g., variations of the tube diameters in a rope and/or vacancies in the tube lattice as observed by HRTEM [12]. We suggest that the decrease of G as the diameter increases may be partly due to the possibility that large ropes contain more imperfections than small ropes. A further reason for the lowering of G is the absence of registry between neighboring tubes induced by variations in tube diameter and helicity. It is worth noting that even for graphite no theory gives a complete description of interplane forces [18], increasing the need for direct measurements.

At first sight, the low shear modulus of SWNT ropes is bad news for potential applications such as reinforcement of materials. However, one may take advantage of the low shear stiffness of nanoropes, for example, in applications where a large damping is required. Incorporation of lamellar graphite in cast iron increases the damping capacity by orders of magnitude [19]. In this case, the presence of glissile dislocations, which decreases the shear modulus, is essential to increase friction between sheets. The low value of G in SWNT ropes suggests, by analogy with lamellar graphite, that imperfections might increase friction between nanotubes, inducing a large damping capacity, especially for large ropes.

In conclusion, we determined both the elastic and the shear moduli for SWNT ropes. From small diameter and long ropes we deduced an elastic modulus of about 1 TPa. Our AFM measurements thus confirm that carbon nanoropes are high-modulus fibers but with an unexpectedly low shear modulus ($G \approx 1$ GPa). This should be taken into account in the design of nanorope-based composite materials. It would be particularly interesting to cross-link the nanotubes in a rope, for example, by irradiation or chemical methods, to increase the rigidity of a rope.

We thank G. Beney (EPFL) for polishing the filters, as well as the CIME-EPFL for access to the electron

microscopes. We also acknowledge G. Gremaud (EPFL) for enlightening discussions. This work was supported by the Swiss NSF.

*Email address: jean-paul.salvetat@epfl.ch

- [1] J.W.G. Wildoer, L.C. Venema, A.G. Rinzler, R.E. Smalley, and C. Dekker, *Nature (London)* **391**, 59 (1998); T.W. Odom, J.-L. Huang, P. Kim, and C.M. Lieber, *Nature (London)* **391**, 62 (1998).
- [2] B. Yakobson, C.J. Brabec, and J. Bernholc, *Phys. Rev. Lett.* **76**, 2511 (1996).
- [3] M.R. Falvo, G.J. Clary, R.M. Taylor II, V. Chi, F.P. Brooks, Jr., S. Washburn, and R. Superfine, *Nature (London)* **389**, 582 (1997).
- [4] M.M.J. Treacy, T.W. Ebbesen, and J.M. Gibson, *Nature (London)* **381**, 678 (1996).
- [5] E.W. Wong, P.E. Sheehan, and C.M. Lieber, *Science* **277**, 1971 (1997).
- [6] J.-P. Salvetat *et al.*, *Adv. Mater.* (to be published).
- [7] C.F. Cornwell and L.T. Wille, *Solid State Commun.* **101**, 555 (1997).
- [8] J.P. Lu, *Phys. Rev. Lett.* **79**, 1297 (1997).
- [9] The SWNTs were produced by arc discharge under a static pressure of helium (500 mbar) using pure graphite electrodes 20 mm (cathode) and 5 mm (anode) in diameter. A 3 mm hole was drilled in the anode and filled with a graphite-Ni-Y mixture with weight proportion 2:1:1. The voltage and current used were approximately 25 V and 100 A. The nanotubes were predominantly found in the webs, as opposed to the cathodic deposit. See also W.K. Maser *et al.*, *Synth. Met.* **77**, 243 (1996).
- [10] The metal catalyst was removed to a great extent by refluxing the arc-discharge webs in nitric acid.
- [11] E.D. Obratsova, J.-M. Bonard, and V.L. Kuznetsov, in *Proceedings of the 12th IWEPNM (AIP, New York, to be published)*.
- [12] A. Thess *et al.*, *Science* **273**, 483 (1996).
- [13] J.M. Gere and S.P. Timoshenko, in *Mechanics of Materials* (PWS-KENT, Boston, 1990).
- [14] This strong adhesion was clearly demonstrated using a rigid cantilever exerting large lateral forces on the suspended portions of the ropes, resulting in high lateral deflections. Under these conditions, no displacement was observed on the portion lying on the membrane. See also Ref. [6].
- [15] A. Zettl (private communication), see also N.G. Chopra and A. Zettl, *Solid State Commun.* **105**, 297 (1998).
- [16] J. Tersoff and R.S. Ruoff, *Phys. Rev. Lett.* **73**, 676 (1994).
- [17] E. Hernandez, C. Goze, P. Bernier, and A. Rubio, *Phys. Rev. Lett.* **80**, 4502 (1998).
- [18] B.T. Kelly, in *Physics of Graphite* (Applied Science, London, 1981).
- [19] E. Plénard, *Fonderie* **177**, 419 (1960); H.T. Angus, *Cast Iron: Physical and Engineering Properties* (Butterworths, London, 1976), 2nd ed.